forests

MDPI

Article

Optimum Phenological Phases for Deciduous Species Recognition: A Case Study on *Quercus acutissima* and *Robinia pseudoacacia* in Mount Tai

Xiao Liu [1,2,3], Ling Wang [3,4,*], Langping Li [1], Xicun Zhu [3,4], Chunyan Chang [3,4] and Hengxing Lan [1,5,*]

1 State Key Laboratory of Resources and Environmental Information System, Institute of Geographic Sciences and Natural Resources Research, Chinese Academy of Sciences, Beijing 100101, China; liuxiao@lreis.ac.cn (X.L.); lilp@lreis.ac.cn (L.L.)
2 University of Chinese Academy of Sciences, Beijing 100049, China
3 College of Resources and Environment, Shandong Agricultural University, Tai'an 271018, China; zxc@sdau.edu.cn (X.Z.); chyan0103@163.com (C.C.)
4 National Engineering Research Center for Efficient Utilization of Soil and Fertilizer Resources, Shandong Agricultural University, Tai'an 271018, China
5 School of Geological Engineering and Geomatics, Chang'an University, Xi'an 710064, China
* Correspondence: lingwang@sdau.edu.cn (L.W.); lanhx@lreis.ac.cn (H.L.)

Abstract: Tree species recognition is important for remote–sensing mapping and dynamic monitoring of forest resource. However, the complex phenological cycle poses a challenge to remote–sensing recognition of deciduous tree species in mountainous areas, and the selection of temporal phase is particularly important to improve recognition accuracy. Multispectral images of Ziyuan–1 02C (ZY–1 02C) and Ziyuan–3 (ZY–3) at three phenological phases of spring, autumn and winter (12 May, 29 September and 7 December, recorded as $T_{5–12}$, $T_{9–29}$ and $T_{12–7}$) are selected to optimize sensitive spectral indices. Support vector machine (SVM) and maximum likelihood model (MLE) are constructed to explore the optimum phase of recognizing on *Quercus acutissima* (*O. acutissima*) and *Robinia pseudoacacia* (*R. pseudoacacia*) in Mount Tai. The results showed the average spectral reflection intensity of *O. acutissima* was higher than that of *R. pseudoacacia* Compared to other phenological periods, the most significant spectral differences between *O. acutissima* and *R. pseudoacacia* were found in the spring (12 May), which was identified as the optimum phenological phase. Band 4 is the most sensitive band in all the three phases for the tree species recognition. Moreover, the overall recognition accuracy of deciduous tree species on 12 May reached 89.25%, which was significantly higher than the other two phases. On 12 May, the recognition accuracies of SVM based on sensitive spectral indices of up to 93.59% for *O. acutissima* and 85.44% for *R. pseudoacacia*, were higher overall than that of the MLE. Sensitive spectral indices introduced were shown to significantly improve the recognition accuracy for tree species over a single sensitive band. The study is expected to facilitate the precise recognition and forestry management on Mount Tai.

Keywords: phenological phases; deciduous species; remote–sensing recognition; support vector machine; Mount Tai

Citation: Liu, X.; Wang, L.; Li, L.; Zhu, X.; Chang, C.; Lan, H. Optimum Phenological Phases for Deciduous Species Recognition: A Case Study on *Quercus acutissima* and *Robinia pseudoacacia* in Mount Tai. *Forests* **2022**, *13*, 813. https://doi.org/10.3390/f13050813

Academic Editor: Herminia García-Mozo

Received: 25 March 2022
Accepted: 18 May 2022
Published: 23 May 2022

1. Introduction

Mount Tai, located in the North China Plain, is the highest mountain in Shandong. It is a famous scenic tourist area in China and a national key cultural relics protection unit, and has the title of World Geopark as a dual heritage of culture and nature in the world. Mount Tai is a typical warm temperate deciduous broad–leaved forest area. The rich plant resources make it a special mountainous area with the most diverse vegetation and the largest number of endemic plant species in Shandong Province [1]. The rapid and precise recognition of deciduous tree species on Mount Tai is an extremely necessary component for efficient forest management, and the selection of the optimal phenological phase is

the foundation for improving the accuracy of vegetation recognition [2]. Traditional field investigation and aerial photography interpretation methods are extremely difficult to use for identifying the Mount Tai tree species, especially in a short time, due to the complicated terrain and inconvenient traffic. Multispectral remote sensing has advantageous features such as macroscopical, short period and repeatable, which can accurately recognize on surface forest features by image spectral and texture data [3]. Widely used multispectral remote sensing provides technical support for tree species identification on Mount Tai [4–6].

The optimum phenological phase is the one that is optimally selected to have the most relevant and distinctive spectral features for recognizing the target vegetation by attenuating the interference of other feature information [7]. Optimal phenological phase selection has been studied by scientists for the recognition of various vegetation species [8,9]. For example, estimation of optimal phase for three major crops (rice, corn and soybean) was established by Owen Ho et al. [10], based on the NDVI time series data from China HJ–1 satellite CCD images and smoothed by wavelet transform filter. The seasonally variable spectral characteristics of the canopies of nine major tree species in the Xiaoxing'anling in the visible and near–infrared bands were analyzed by Xu Guangcai et al. [11], collected by the ASD FieldSpec portable spectrometer, while the optimal band and period patterns for tree species identification were explored. It was found that the spectral characteristics of deciduous trees changed with seasonal regularity, while those of evergreen trees did not change significantly during the year. Reflectance of Landsat 8 image at optimal temporal were combined with NDVI time series by rough set method to classify cotton, the classification accuracy was greatly improved compared to the unoptimized NDVI time series [12].

Support vector machines, maximum likelihood estimation, decision trees, and neural networks are some of the most widely used methods for remote–sensing recognition of tree species and have achieved some recognition results [13–16]. Among the methods, decision tree is often used for high spatial resolution airborne multispectral image classification, such as single urban tree species with longitudinal profiles, and six major tree species (maple, ash, birch, oak, spruce, and pine) campus trees at the University of York were successfully recognized with an accuracy of over 80% [5]. Maximum likelihood, neural network, mahalanobis distance and support vector machine methods were separately used to recognize four major cultivar fruit trees (walnut, jujube, pear and apple) in southern Xinjiang basin, China, based on spectral and texture data from high–resolution remote–sensing images. Support vector machine was found to be the best classification method for the four fruit tree species with the highest recognition accuracy of 69.71% [17]. Support vector machines were also successfully applied to the species identification of *Myrtle Beech*, a dominant tree species in Australian cold temperate rainforests, and its neighboring species using LiDAR scan data, with the overall accuracy of 92.8% showing the significant advantage of support vector machines over other classification methods [18]. The spectral feature data from Landsat–8 OLITIRS were input into the support vector machine to identify forest types in Wangqing natural forest area, Jilin Province, and it was found that the support vector machine with radial basis kernel function had the best classification accuracy, and the overall classification accuracy exceeded 80%, but only achieved rough classification of broadleaf, coniferous, and mixed coniferous–broadleaf forests and lacked classification of deciduous interspecies [19]. In general, the previous researches showed that the support vector machine has a better recognition effect for tree species by remote–sensing technology. However, only a rough classification of forest types was carried out, while the classification accuracy of specific tree species still needs to be improved. Bands reflectance was widely and directly used to recognize on tree species in existing researches with the multi–spectral remote sensing. However, the spectral indices are expected to enlarge the slight difference between the spectrum and improve the recognition accuracy [20].

Quercus acutissima (*O. acutissima*) and *Robinia pseudoacacia* (*R. pseudoacacia*), as the most representative tree species of deciduous broad–leaf forest in warm temperate zone, having similar phenological periods and the largest distribution area on Mount Tai, are

selected as recognition tree species [21,22]. Multispectral images of Ziyuan–1 02C (ZY–1 02C) and Ziyuan–3 (ZY–3) at three phenological phases of spring, autumn and winter (12 May, 29 September and 7 December, recorded as $T_{5–12}$, $T_{9–29}$ and $T_{12–7}$) were selected to optimize sensitive spectral indices. The support vector machine (SVM) and maximum likelihood model (MLE) were constructed to explore the optimum phenological phase of recognizing on *O. acutissima* and *R. pseudoacacia* on Mount Tai.

2. Data and Methods

2.1. Study Area

Our study area is located on Mount Tai (116°50′~117°12′ E, 36°11′~36°31′ N), central location of Shandong Province, China (Figure 1). Mount Tai has the highest altitude of 1545 m, and the total area of 11,732.96 hm^2. The area belongs to the warm temperate continental monsoon climate zone. The vertical zonal character leads to the difference in annual average temperature between the mountain summit and base, at 5.3 °C and 12.8 °C, respectively. The mean annual precipitation is 1124.6 mm, mainly occurs from June to August, and the annual relative humidity is 63%.

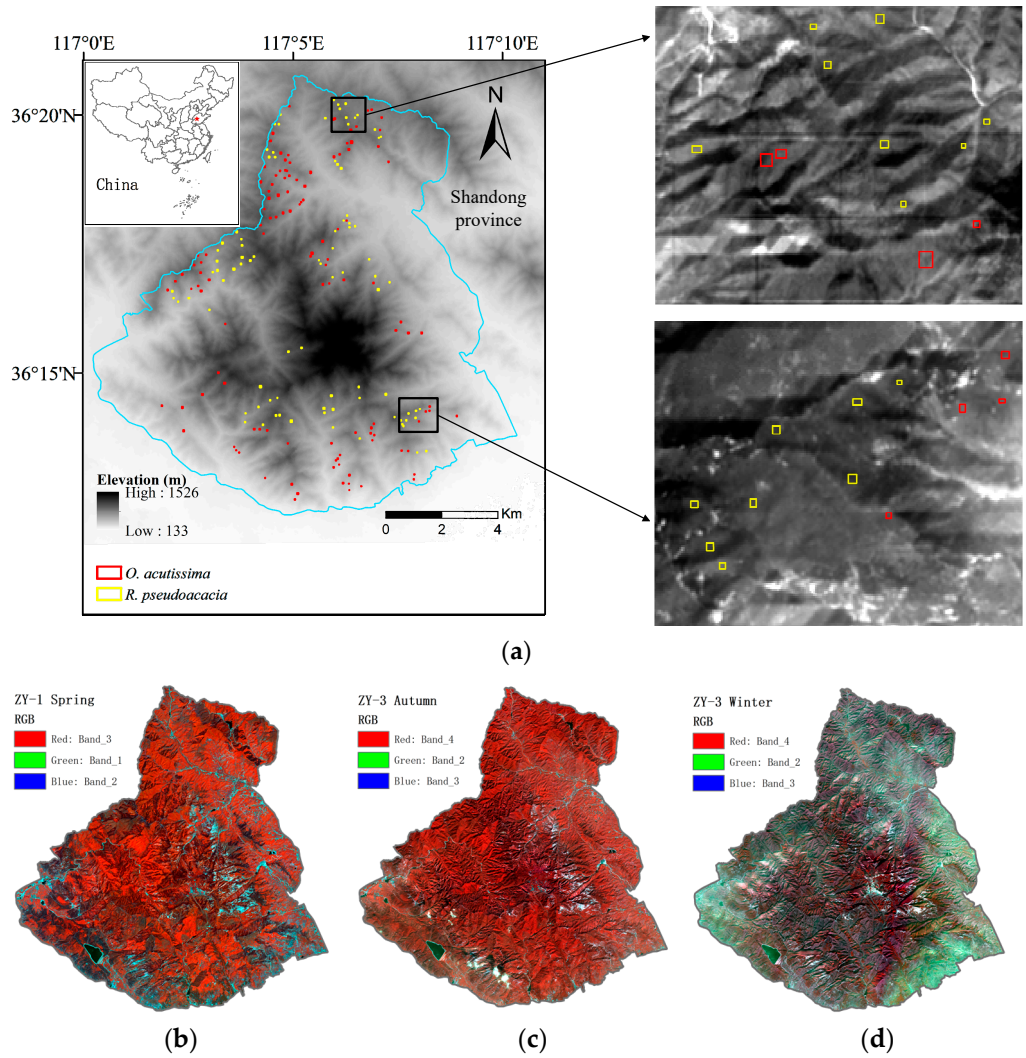

Figure 1. (**a**) Location map of the study region and images of the sample area. (**b**) Spring image; (**c**) autumn image; (**d**) winter image.

Mount Tai is a huge ecological barrier and an important germplasm resource bank because of the abundant plant resources. The vegetation coverage rate is over 90%, in which the woodland reaches 81.5% and nearly 10,000 hm^2. The deciduous vegetation

changes significantly with the four distinct seasons. *O. acutissima* stand has a long growth cycle, most of which is nearly mature generation forest. *R. pseudoacacia* was introduced to Mount Tai in the 1920s, and has now gradually evolved into naturally–regenerated coppice plantations. The two tree species are mainly distributed along an altitudinal gradient about from 400 to 1000 m above sea level in Mount Tai.

2.2. Phenologic Characteristics of Tree Species

O. acutissima and *R. pseudoacacia* have typical phenological characteristics of deciduous species, which are prominently displayed on Mount Tai where the seasons are distinct. The selection of the phenological period of two tree species directly contributes to the effect of remote–sensing recognition. The phenological characteristics of *O. acutissima* and *R. pseudoacacia* throughout the year are shown in Table 1 [23]. In general, the fruit ripening and defoliating periods of *O. acutissima* is one to two months later than those of *R. pseudoacacia*, and the two species show near–synchrony in other phenological periods. In particular, both species are in the flowering period in May, in the significant leaf color change in late September, and in the differential defoliation period in mid–December. In these three phenological phases, the phenological characteristics of *O. acutissima* and *R. pseudoacacia* show distinguishability and differences, and have the advantage of being selected for remote–sensing identification.

Table 1. Key phenological period of *O. acutissima* and *R. pseudoacacia* throughout a year.

Tree Species	Germinating	Leaf Expansion	Flowering	Fruit Ripening	Leaf Color Changing	Defoliating
O. acutissima	Mid to late March	The end of March to early April	Late March to early May	September to October of the next year	Late September to mid October	Late November to the end of December
R. pseudoacacia	Late February to early April	Early to mid April	Mid April to mid May	Mid July to September of the next year	Late September to early October	Mid October to late November

2.3. Multispectral Data

Considering the topographic features of the study area, the phenological characteristics of *O. acutissima* and *R. pseudoacacia*, and the accessibility and applicability of remote–sensing data, a total of three scenes of multispectral remote–sensing images on September 29 and December 7 of Ziyuan–3 (ZY–3) and May 12 of Ziyuan–1 02C (ZY–1 02C) in 2014 were selected for this classification identification. Although the ZY–1 02C multispectral image has three bands, one less than ZY–3, the two images have identical band ranges in green, red, and near–infrared bands (Table 2), so ZY–1 02C was selected to compensate for the lack of the May 2014 image from the ZY–3 remote–sensing satellite. In addition, the spatial resolution of ZY–1 02C image is 10 m, which is slightly lower than that of ZY–3, and the comparative differences in classification effects will be further discussed in the study results. The pretreatment of atmospheric conditioning, geometrical correction, and geometric fine–prediction had been performed on the remote–sensing images before the species recognition. Topographic radiometric correction was particularly performed with multiple validations to reduce the influence of the complex topography of Mount Tai on the recognition results. For the spectral characterization, we consider that the spectral differences are significant in some cases when analyzing the spectral reflectance differences between bands or between different tree species. Between two bands, the band with the larger mean reflectance is more than one times larger than the band with the smaller mean reflectance, which is considered a significant spectral difference between the bands. Between the two tree species, the difference in average reflectance of a band is 20% larger than that of the tree species with smaller average reflectance, which is considered a significant spectral difference between the tree species.

Table 2. Image parameters.

		B_1 (Blue)/μm	B_2 (Green)/μm	B_3 (Red)/μm	B_4 (Near Infrared)/μm	Spatial Resolution/m
Multispectral image	ZY–3	0.45–0.52	0.52–0.59	0.63–0.69	0.77–0.89	5.8
	ZY–1 02C	—-	0.52–0.59	0.63–0.69	0.77–0.89	10

Note: ZY–1 02C bands are numbered as 2, 3, 4 bands to facilitate the comparison.

2.4. Sample Selection

Vegetation surveys were conducted in 2014, consistent with the year of remote–sensing recognition images. The setup of each plot in the plant–species investigation was based on the principle of distribution uniformity and tree species typicality. For further systematic and rational sampling, the range of altitude was divided into 200 m bands. The sample areas of each tree species were selected in three elevation bands with latitudes of 400–600 m, 600–800 m, and 800–1000 m, respectively. Considering the altitudinal distribution characteristics of *O. acutissima* and *R. pseudoacacia* in Mount Tai, the number of sample areas in these three altitude zones was selected in the ratio of 1:3:2. The sampling sites were representative of typical tree types in each altitudinal band and away from clough and slope crest, large stream gullies and rocky outcrops. A total of 119 sample areas of *O. acutissima* and 88 sample areas of *R. pseudoacacia* were finally selected, all of which were rectangular in shape, as shown in Figure 1. Regarding the sample area of *O. acutissima*, the smallest is 25.82 m^2, the largest is 3593.88 m^2, the total area of all *O. acutissima* sample areas is 118,798.77 m^2, the average area is 998.31 m^2; Regarding the sample area of *R. pseudoacacia*, the smallest is 114.43 m^2, the largest is 3596.80 m^2, the total area of all *R. pseudoacacia* sample areas is 77,175.19 m^2, the average area is 876.99 m^2. Based on the classification advantages of remote–sensing multispectral image data, pixel points were chosen as the base unit for the experiment. There were 2550 pixels in *O. acutissima* sample area, and 1635 pixels in *R. pseudoacacia* sample area. According to the difference of the spectral index of each species, equidistant sampling was applied to select 2/3 pixels as modeling samples (1700 of *O. acutissima*, 1090 of *R. pseudoacacia*) and 1/3 pixels as validation samples (850 of *O. acutissima*, 545 of *R. pseudoacacia*) to construct the SVM and MLE models, respectively. The sample area groups of *O. acutissima* and *R. pseudoacacia* located on the northern shady slope and southern sunny slope of Mount Tai, respectively, were enlarged to clearly show the distribution of the sample areas. Both tree species sample areas are dominated by typical pure forest areas in each altitudinal band and away from clough and slope crest, large stream gullies and rocky outcrops, as shown in Figure 1a.

2.5. Recognition Algorithm

The support vector machine algorithm (SVM), first proposed by Vapnik in 1995 [24], is a pattern recognition method based on statistical learning theory that enables classification and regression analysis through data training. SVM has the advantage of eliminating overfitting and is robust to noise [25,26], and is particularly suitable for classification applications on multidimensional and high–dimensional data [26–29]. The key of SVM classification lies in the kernel function, which maps the sample data from the original feature space to the high–dimensional feature space and finds the optimal hyperplane in the feature space to maximize the classification interval, thus achieving accurate classification of sample data [24]. The kernel functions of SVM classification include Linear Kernel, Polynomial Kernel, Radial Basis Function (RBF), Sigmoid Kernel [30]. The SVM classifier constructed by RBF was studied and proved to have better classification advantages, and was used in this study [31].

Maximum likelihood estimation (MLE) is a classification method that uses a maximum likelihood function to estimate the parameters of a hypothetical probability distribution given training data. MLE is the most traditional and commonly used method for statistical classification due to its intuitive and flexible advantages of statistical logic. The MLE model was constructed in this study as a control to validate the SVM recognition results [32].

2.6. Sensitive Spectral Indices

Mathematical calculation methods were used to construct spectral indices based on the spectral reflectance extracted from the image–sample areas, and the corresponding formulations are shown in Table 3. The total number of spectral indices constructed for each phenological phase is 90 for $T_{5–12}$, 166 for $T_{9–29}$, and 166 for $T_{12–7}$. The spectral indices were analyzed and screened to construct support vector machines and maximum likelihood models for the recognition of *O. acutissima* and *R. pseudoacacia* Firstly, a multi–categorical logistic regression model was used to analyze the correlation between spectral indices and tree species types, where spectral indices were quantitative independent variables and tree species types were qualitative dependent variables. The 10 spectral indices with the highest correlation coefficients were determined to be sensitive spectral indices. Then, these 10 sensitive spectral indices were used separately to construct a one–dimensional model, on the one hand, and combined to construct a 10–dimensional model, on the other hand. Finally, the three spectral indices with the highest recognition accuracy among the 10 one–dimensional models were selected as the best sensitive spectral indices, which were further used to construct the three–dimensional models. The recognition accuracies of different models on *O. acutissima* and *R. pseudoacacia* in different time phases were compared and analyzed to select the optimum phenological phase. It should be noted that in order to reduce the effect of altitude on vegetation phenology on Mount Tai, the spectral data of the three phenological zones were extracted separately to construct spectral indices and applied to classification models, and the mean value of recognition accuracy of the three phenological zones for each tree species was calculated as the final accuracy of the species.

Table 3. Construction formulations of spectral indices.

Single Band		Multi–Band		
B_i^2	$B_i^{1/3}$	$B_i \pm B_j$	$lnB_i/(B_i \pm B_j)$	$(B_iB_j)/(B_i + B_j)$
B_i^3	e^{Bi}	B_iB_j	$(B_i \pm B_j)/e^{Bi}$	$(B_i - B_j)/(B_i + B_j)$
$B_i^{0.5}$	lnB_i	B_i/B_j	$(B_i/B_j)/(B_i \pm B_j)$	$(B_i - B_j)/(B_iB_j)$

Note: B_i, B_j (i, j = 1, 2, 3, 4): Reflectance of image band.

3. Results

3.1. Spectral Characteristics

Box–and–whisker plots were plotted to represent statistical features such as minimum, maximum, quartile, and mean values of spectral reflectance, as shown in Figure 2. The data features of standard deviation and mean values were used as the focus for analyzing the spectral characteristics of each phenological phase. The reflectance values of the three temporal phases of *O. acutissima* and *R. pseudoacacia* showed different characteristics, as shown in Figure 2. The overall reflectance values of $T_{5–12}$ were higher than those of the other two temporal phases, and the differences in reflectance between bands were obvious, such as B_4 was significantly higher than B_2 and B_3. Similarly, the B_4 reflectivity of $T_{9–29}$ is significantly higher than the other three bands. The reflectance values of the four bands of $T_{12–7}$ were less different, and the average reflectance was between 0.04 and 0.1. Among the two species, the average reflectance of *O. acutissima* was higher than that of *R. pseudoacacia*, especially in B_4.

The differences in the spectral reflectance of *O. acutissima* and *R. pseudoacacia* indicated that the largest difference in reflectance between the two species was at $T_{5–12}$ B_4 ($\overline{X} = 0.0958$), although it has a little higher standard deviation ($\sigma_{Q.A.} = 0.0278$, $\sigma_{R.P.} = 0.0425$). Secondly, the reflectance of the two species also had a clearly distinguishable difference in $T_{5–12}$ B_3 ($\overline{X} = 0.0242$), and the B_3 reflectance data set had less dispersion ($\sigma_{Q.A.} = 0.0067$, $\sigma_{R.P.} = 0.0145$), and it can be found that $T_{5–12}$ B_3 and B_4 showed better identification potential for *O. acutissima* and *R. pseudoacacia* The spectral reflectance of the two species in the $T_{9–29}$ temporal phase did not show significant differences in the other three bands

($\overline{X}_{B1} = -0.0038$, $\overline{X}_{B2} = -0.0033$, $\overline{X}_{B3} = -0.0040$), except for B_4 ($\overline{X} = 0.0202$). However, the spectral reflectance data set of B_4 had excessive dispersion ($\sigma_{Q.A.} = 0.0206$, $\sigma_{R.P.} = 0.0305$), which could easily cause confusion in the tree species identification process. Similar to $T_{9–29}$, the differences of spectral reflectance between the two tree species in the $T_{12–7}$ temporal phase were not significant in B_1, B_2 and B_3 ($\overline{X}_{B1} = -0.0017$, $\overline{X}_{B2} = -0.0025$, $\overline{X}_{B3} = -0.0080$), but showed significant differences in B_4 ($\overline{X} = 0.0237$), and the dispersion of the B_4 reflectance data set was relatively small ($\sigma_{Q.A.} = 0.0169$, $\sigma_{R.P.} = 0.0135$). Thus, it appears that $T_{12–7}$ B_4 is second only to $T_{5–12}$ B_3 and B_4 in terms of suitability for the identification of *O. acutissima* and *R. pseudoacacia*.

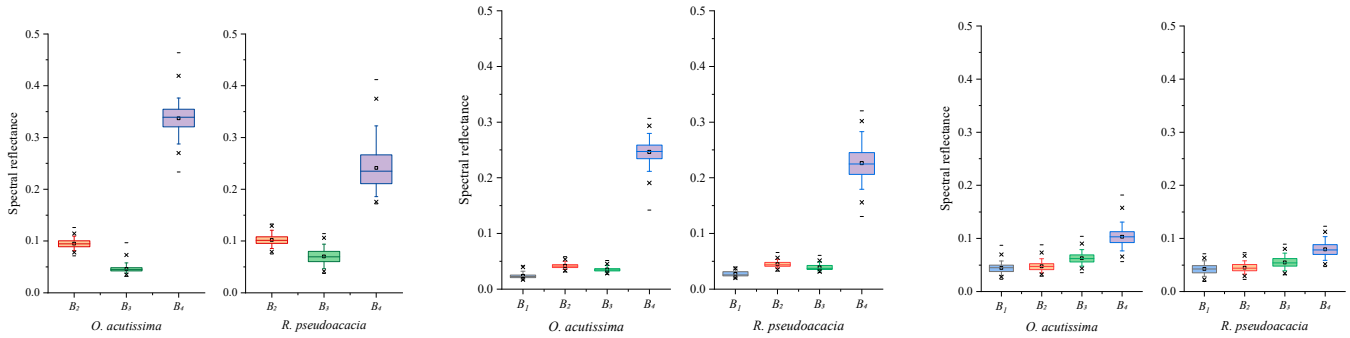

(a) $T_{5–12}$ (b) $T_{9–29}$ (c) $T_{12–7}$

Figure 2. Spectral reflectance of each band at different phenological phases.

3.2. Sensitive Band and Sensitive Spectral Index

The correlations between spectral indices and tree species types were analyzed and the 10 sensitive spectral indices with the highest correlation coefficients were identified as in Table 4. We further analyzed the obtained correlation coefficients by referring to the range of correlation coefficients (rounded to two decimal places) proposed in the relevant literature into eight categories, i.e., 0.00 to ±0.30, ±0.30 to ±0.50, ±0.50 to ±0.80, and ±0.80 to ±1.00 indicating slight, real, significant, and high positive or negative correlations, respectively, [33,34].

Table 4. Sensitive spectral indices of recognition for *O. acutissima* and *R. pseudoacacia*.

		$T_{5–12}$	**$T_{9–29}$**	**$T_{12–7}$**
Sensitive spectral indies	X_1	$(B_2 - B_3)/(B_2B_3)$	$B_2 - B_4$	B_4/B_3
	X_2	$(B_3 - B_4) \times (B_3 + B_4)$	$(B_1 - B_4)/(B_1B_4)$	$(B_4/B_3)/(B_4 - B_3)$
	X_3	e^{B4}	$(B_4 - B_2)/(e^{B4})$	$lnB_3/(B_3 - B_4)$
	X_4	lnB_4	$(B_3 - B_4)/(B_3B_4)$	B_3/B_4
	X_5	${B_4}^{1/3}$	$(B_2/B_4)/(B_2 - B_4)$	$lnB_4/(B_4 - B_3)$
	X_6	${B_4}^{0.5}$	$(B_2/B_4)/(B_2 + B_4)$	$B_4 - B_3$
	X_7	$B_2 - B_4$	$(B_3/B_4)/(B_3 + B_4)$	$B_3 - B_4$
	X_8	$B_3 - B_4$	B_2/B_4	$(B_3 - B_4)/(e^{B3})$
	X_9	$(B_3 - B_4)/(e^{B3})$	B_4/B_1	$(B_4 - B_3)/(e^{B4})$
	X_{10}	B_4/B_3	B_4/B_3	$(B_3/B_4)/(B_3 - B_4)$
		$T_{5–12}$	**$T_{9–29}$**	**$T_{12–7}$**
X_1		$(B_2 - B_3)/(B_2B_3)$	$B_2 - B_4$	B_4/B_3
X_2		$(B_3 - B_4) \times (B_3 + B_4)$	$(B_1 - B_4)/(B_1B_4)$	$(B_4/B_3)/(B_4 - B_3)$
X_3		e^{B4}	$(B_4 - B_2)/(e^{B4})$	$lnB_3/(B_3 - B_4)$
X_4		lnB_4	$(B_3 - B_4)/(B_3B_4)$	B_3/B_4
X_5		${B_4}^{1/3}$	$(B_2/B_4)/(B_2 - B_4)$	$lnB_4/(B_4 - B_3)$
X_6		${B_4}^{0.5}$	$(B_2/B_4)/(B_2 + B_4)$	$B_4 - B_3$
X_7		$B_2 - B_4$	$(B_3/B_4)/(B_3 + B_4)$	$B_3 - B_4$
X_8		$B_3 - B_4$	B_2/B_4	$(B_3 - B_4)/(e^{B3})$
X_9		$(B_3 - B_4)/(e^{B3})$	B_4/B_1	$(B_4 - B_3)/(e^{B4})$
X_{10}		B_4/B_3	B_4/B_3	$(B_3/B_4)/(B_3 - B_4)$

Note: B_i (i = 1, 2, 3, 4) represents the band reflectance of images.

The correlation coefficients between different bands and tree species for each phenological phase can be found, as shown in Figure 3, that $T_{5–12}$ B_4 showed the highest correlation among all bands with highly negative correlation, followed by $T_{5–12}$ B_3 with a significant positive correlation, and $T_{9–29}$ B_4 and $T_{12–7}$ B_4 with a significant negative correlation. B_4 was therefore considered the most sensitive band for recognizing *O. acutissima* and *R. pseudoacacia*, especially in $T_{5–12}$, which was initially considered the best phenological phase. Thus, the results of the sensitivity analysis of the bands were found to be consistent to some extent with the conclusions of the analysis of spectral characteristics in Section 3.1. The correlation coefficients between the sensitive spectral indices and tree species indicate that the overall correlation among the three phenological phases was $T_{5–12}$ > $T_{12–7}$ > $T_{9–29}$. $T_{5–12}$ showed an extraordinarily high correlation with the highest coefficient of 0.82. $T_{12–7}$ followed with the highest correlation coefficient of 0.75. $T_{9–29}$ showed a poorer correlation with the highest coefficient of 0.52.

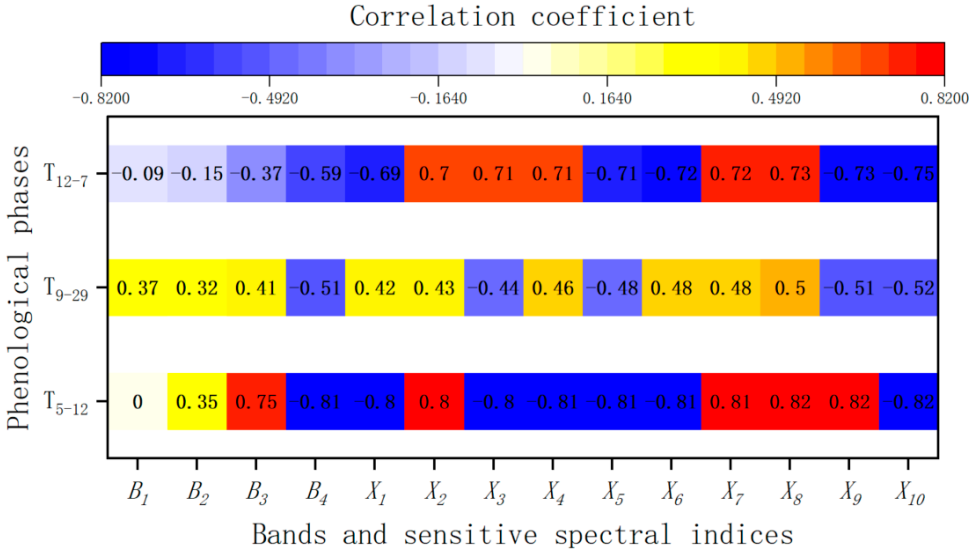

Figure 3. Correlation coefficient between band/sensitive spectral indices and tree species types.

The band composition of the sensitive spectral indices was found to contain all sensitive bands (Table 4). Specifically, among the three phenological phases, seven (X_4–X_{10}) of the ten sensitive spectral indices of $T_{5–12}$ had higher correlation coefficients than the most sensitive band (B_4). Eight (X_3–X_{10}) of the ten sensitive spectral indices of $T_{9–29}$ had higher correlation coefficients than the most sensitive band (B_4). The correlation coefficients of ten sensitive spectral indices (X_1–X_{10}) of $T_{12–7}$ are all higher than the most sensitive band B_4. This indicates that the construction of sensitive spectral indices improved the correlation of spectral information with tree species.

3.3. Recognition Accuracy

To ensure the comparability of the recognition results, the construction parameters of both the one–dimensional and multi–dimensional SVM models were kept consistent, as shown in Table 5. The radial kernel function was selected to construct the SVM model throughout because of its recognized discriminative advantages. The recognition accuracies of SVM and MLE models constructed with sensitive band and sensitive spectral indexes, respectively, for *O. acutissima* and *R. pseudoacacia* are shown in Figure 4. We compared and analyzed the recognition accuracy results of SVM models, including 10–dimensional SVM models constructed by both sensitive bands and sensitive spectral indicators, and 3–dimensional SVM models constructed by the best sensitive spectral indicators. The recognition accuracy is calculated by inputting the validation pixel values as variables into the classification model constructed by modeling pixel values, that is, the testing accuracy, as shown in Figure 4. At the same time, in order to compare the differences in recognition

results between bands and spectral indices, different phenological phases, and different models straightforwardly, the recognition accuracies of *O. acutissima* and *R. pseudoacacia* under the same conditions were averaged and described as the overall recognition accuracy of the two species. MLE model was constructed by the spectrum data of $T_{5–12}$, which was more evidentially proven to be the best recognition phase, for use as the comparison and validation of the SVM recognition results. The recognition accuracy of the univariate sensitive spectral indices constructed by the one–dimensional SVM model was analyzed to yield the best sensitive spectral indices for the three temporal phases of X_5, X_8 and X_9 on $T_{5–12}$; X_5, X_7 and X_8 on $T_{9–29}$; X_3, X_5 and X_{10} on $T_{12–7}$, respectively, (Table 4). The validation accuracy and modeling accuracy are found generally consistent (Figure 4).

Table 5. Model parameters of SVM.

Tree Species	Degree	Gamma	Coef0	Epsilon	C	Nu	Shrinking	P
O. acutissima	3	0.5	0.001	0.001	1	0.5	1	1
R. pseudoacacia	3	0.5	0.001	0.001	1	0.5	1	1

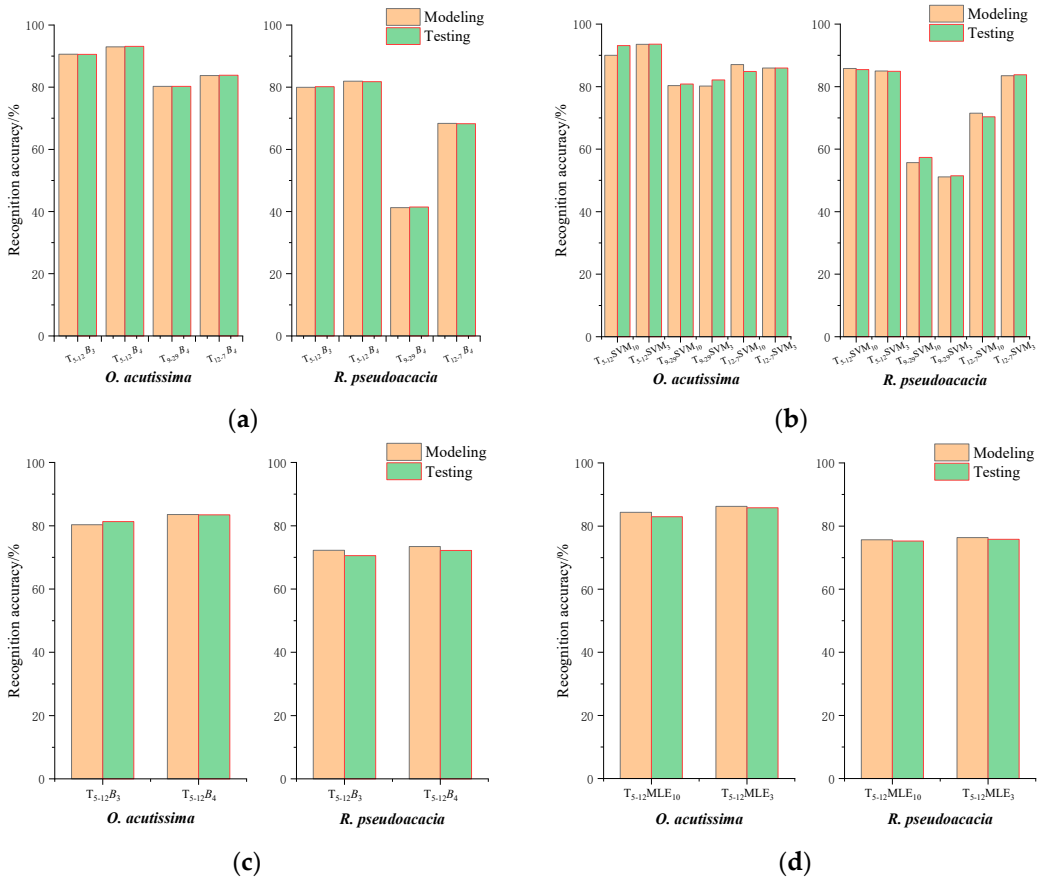

Figure 4. Recognition accuracy of SVM and MLE for *O. acutissima* and *R. pseudoacacia* in different phenological phases. (**a**) SVM with sensitive band; (**b**) SVM with sensitive spectral indices. SVM_3 and SVM_{10} represent three and ten dimensional SVM models constructed by three best sensitive spectral indices and ten sensitive spectral indices, respectively; (**c**) MLE with sensitive band; (**d**) MLE with sensitive spectral indices. MLE_3 and MLE_{10} represent three and ten dimensional MLE models constructed by three best sensitive spectral indices and ten sensitive spectral indices, respectively.

The recognition accuracy was analyzed and it was found that the model constructed with sensitive spectral indices outperformed that with sensitive bands, both for *O. acutissima* and *R. pseudoacacia* Firstly, for *O. acutissima*, the 3–dimensional SVM model (SVM_3) had the

highest accuracies on all three phases. SVM_3 on $T_{5–12}$ was 93.59%, higher than B_3 (90.53%) 3.06% and higher than B_4 (93.12%) 0.46%; SVM_3 on $T_{12–7}$ was 85.94%, higher than the B_4 (83.82%) 2.12%; SVM_3 on $T_{9–29}$ was 82.12%, higher than B_4 (80.24%) 1.88%. Secondly, for *R. pseudoacacia*, the 10–dimensional SVM model (SVM_{10}) had the highest accuracy on $T_{5–12}$ and $T_{9–29}$, and the SVM_3 had the highest accuracies on $T_{12–7}$. SVM_{10} on $T_{5–12}$ was 85.44%, higher than B_3 (80.12%) 5.32% and higher than B_4 (81.77%) 3.67%; SVM_{10} on $T_{9–29}$ was 57.37%, higher than B_4 (41.47%) 15.90%; SVM_3 on $T_{12–7}$ was 83.78%, higher than B_4 (68.26%) 15.52%, as shown in Figure 4a,b. The overall recognition accuracy of B_4 for *O. acutissima* and *R. pseudoacacia* on $T_{5–12}$ was higher than that of B_3. The B_4 of $T_{5–12}$ was confirmed to be the most sensitive band in this phenological phase ($T_{5–12}$), the same for $T_{9–29}$ and $T_{12–7}$.

The recognition efficiency of *O. acutissima* was found to be apparently higher than that of *R. pseudoacacia* As example with the SVM model constructed by sensitive spectral indices, the maximum recognition accuracy of *O. acutissima* was 93.59 %, derived from the SVM_3 constructed by $T_{5–12}$ spectral indices; the minimum was 80.82% derived from the SVM_{10} constructed by $T_{9–29}$ spectral indices. However, the maximum recognition accuracy of *R. pseudoacacia* was 85.44 %, derived from SVM_{10} constructed by $T_{5–12}$ spectral indices; and the minimum was 51.50 %, derived from SVM_3 constructed by $T_{9–29}$ spectral indices. The overall recognition accuracy of SVM_3 (84.79%) was higher than that of SVM_{10} on $T_{12–7}$ (78.45%), but similar on $T_{5–12}$ and $T_{9–29}$. The recognition models constructed by spectral information obtained from the three phenological phases were compared and it was found that the recognition accuracy of 12 May under all model construction conditions showed a predominantly high level, and was determined as the optimum phenological phase for the recognition of *O. acutissima* and *R. pseudoacacia* The maximum likelihood estimation model was constructed based on the sensitivity band and the sensitive spectral indices of $T_{5–12}$ for comparison with SVM, as shown in Figure 4c,d. The recognition accuracy of the MLE for both *O. acutissima* and *R. pseudoacacia* on $T_{5–12}$ was lower than that of the SVM under the same model construction conditions. For example, the overall accuracy of the MLE (76.11% and 78.16%) based on B_3 and B_4 from $T_{5–12}$ was 9.18% and 9.30% lower than that of the SVM (85.29% and 87.46%), respectively. The overall accuracy of the MLE_{10} (79.57%) and MLE_3 (81.06%) on $T_{5–12}$ were 9.02% and 8.19% lower than that of the SVM_{10} (88.59%) and SVM_3 (89.25%), respectively. The application of the MLE model contributively demonstrated that B_4 was the most sensitive band and the introduced sensitive spectral indices have a competitive improvement in recognition accuracy for *O. acutissima* and *R. pseudoacacia* compared to the sensitive band.

4. Discussion

Mean spectral reflectance was selected to recognize *O. acutissima* and *R. pseudoacacia* in this study. The effect of elevation on vegetation phenology could not be ignored. Therefore, we tried to reduce the influence of elevation on tree species recognition results in three aspects: vegetation selection, sample area delineation and data modeling. We compared in detail the recognition results for *O. acutissima* and *R. pseudoacacia* within each elevation band and found that the two species could be identified by the spectral differences between the two species within the same elevation band, while the average reflectance of the combined multiple elevation bands amplified the spectral differences between the two species to some extent. The explanation for the spectral differences between the two species being amplified by the integration of spectral variations from multiple elevation bands has not been clearly revealed, but the delineation at finer elevation band scales will be a promising research direction for future tree species recognition based on remote–sensing techniques.

The conclusion that spring $T_{5–12}$ is recommended as the best phenological period for identifying *O. acutissima* and *R. pseudoacacia* in this study is derived with evidence, while there is a degree of uncertainty as the image data used were based on different satellites. Specifically, the spring $T_{5–12}$ image data were obtained from ZY–1 02C, and the autumn $T_{9–29}$ and winter $T_{12–7}$ image data were obtained from ZY–3. The spatial resolution of $T_{5–12}$ is 10 m, which is lower than ZY–3′s 5.8 m, and the multispectral bands are three,

one less than ZY–3, although the three available bands have exactly the same spectrum, as shown Table 2. The relatively lower spatial resolution and fewer bands compared to ZY–3 may potentially reduce the remote–sensing recognition competence of the spring $T_{5–12}$ multispectral image, yielding a lower recognition accuracy for *O. acutissima* and *R. pseudoacacia* Nevertheless, ZY–1 02C image in $T_{5–12}$ phenology phase was found to have higher recognition accuracy than ZY–3 on *O. acutissima* and *R. pseudoacacia* in the obtained results, even with the potentially reduced recognition capability. This is a conclusive and substantial confirmation that $T_{5–12}$ is the best phenological phase for the recognition of *O. acutissima* and *R. pseudoacacia* among the three phases.

Spring is identified as the best recognition phase presumably due to the large canopy morphology differences in leaves and flowers between *O. acutissima* and *R. pseudoacacia*, especially the flowering morphology, as shown in Table 1. The leaf morphology of *O. acutissima* is lanceolate and clustered, with the single leaf is 8–19 cm long and 2–6 cm wide [35]; the leaf morphology of *R. pseudoacacia* is ovate, dichotomous alternate or opposite, with the single leaf measuring 2–5 cm long and 1.5–2.2 cm wide, and the pinnate compound leaf measuring 10–25 cm long. Both species had finished the leaf unfolding on 12 May, and the differences in single leaf size and morphology, as well as the differences in leaves compound structure between the two species were displayed amply. In addition, the flowers of *O. acutissima* have already faded in the middle and early May, while the flowers of *R. pseudoacacia* are in full bloom. The morphological appearance of *R. pseudoacacia* flowers is characterized by the distinguishable white papilionaceous corolla, racemes and axillary inflorescences [36]. Therefore, both the leaves and flowers may be the dominant morphological traits recognized by remote–sensing methods.

The differences in crown width and tree height may also be one of the explanations for the spectral differences between the two species of *O. acutissima* and *R. pseudoacacia* However, differences in crown width and height are more determined by the elevation zone, slope direction, and age of the tree species. For example, under similar environmental conditions, the older the tree the greater the canopy width and height. Therefore, differences in tree height and canopy width are not sufficiently accounted for by the differences in spectral variation among tree species when the environmental conditions such as growing location and age are not negligible. Consequently, when the structural features of crown width and height are specifically designed to extract spectral variation for accurate classification of broad–leaved tree species, further investigation of background conditions such as age and elevation zone of the target tree species is a necessary prerequisite.

Compared with sensitive bands, the SVM constructed by sensitive spectral indices improved the recognition accuracy of *R. pseudoacacia* more than that of *O. acutissima*, which may imply that the recognizability of tree morphological traits potentially implicates higher remote–sensing recognition accuracy. For example, *R. pseudoacacia* improved the recognition accuracy more than *O. acutissima* in the May 12 phase (Figure 4a,b), probably because *R. pseudoacacia* was in full bloom at this phase, while the flowers of *O. acutissima* had already fallen, as shown in Table 1 [23,36]. In addition, the few numbers of tree species, *O. acutissima* and *R. pseudoacacia*, may result in limited generalizability of the recognition results, the selection of the optimum phenological phase for deciduous broad–leaved trees should include more species in the future studies.

5. Conclusions

Phenological phases are particularly important for remote–sensing recognition of deciduous tree species in mountainous areas. Multispectral images at three phenological phases of spring, autumn and winter are selected to optimize sensitive spectral indices and construct SVM and MLE recognition models. The optimum phase for recognizing main deciduous tree species on Mount Tai are explored in this study. We showed the average spectral reflection intensity of *O. acutissima* was higher than that of *R. pseudoacacia* Compared to other phenological periods, the most significant spectral differences between *O. acutissima* and *R. pseudoacacia* were found in the spring (12 May), which was identified as

the optimum phenological phase. Moreover, the overall recognition accuracy of deciduous tree species on 12 May reached 89.25%, which was significantly higher than the other two phases. Band 4, followed by band 3, are the most sensitive bands in all the three phases for tree species recognition. On 12 May, the recognition accuracies of SVM based on sensitive spectral indices of up to 93.59% for *O. acutissima* and 85.44% for *R. pseudoacacia*, overall higher than that of the MLE. Sensitive spectral indices introduced were shown to significantly improve the recognition accuracy for tree species over a single sensitive band. The study is expected to facilitate the precise recognition and forestry management on Mount Tai.

Author Contributions: X.L. wrote the paper. L.W. provided the research data, planned the research, guided the research framework. L.L. provided the English language editing. X.Z. collected the sample data. C.C. analyzed the satellite image data. H.L. improved research methodology and provided project funding support. All authors have read and agreed to the published version of the manuscript.

Funding: This research was funded by [L.W.] grant number [National Natural Science Foundation of China (Grant No. 42171378 and 41877003)] And The APC was funded by [National Natural Science Foundation of China (Grant No. 42041006) and Strategic Priority Research Program of the Chinese Academy of Sciences (Grant No. XDA23090301)].

Institutional Review Board Statement: Not applicable.

Informed Consent Statement: Not applicable.

Data Availability Statement: The experimental data were measured according to the test specifications, which can be used for further analysis.

Conflicts of Interest: The authors declare no conflict of interest.

References

1. Su, Y.; Li, J.; Qiu, J.; Jin, Z.; Fang, X.; Chao, Y.; Wang, J.; Zhou, H. Current situation investigation and analysis of medicinal plant resources in Mount Tai area. *Chin. Wild Plant Resour.* **2018**, *37*, 1006–9690.
2. Huanxue, Z.; Xin, C.; Qiangzi, L.; Miao, Z.; Xinqi, Z. Research on crop identification using multi-temporal NDVI HJ images. *Remote Sens. Technol. Appl.* **2015**, *30*, 304–311.
3. Lehmann, E.A.; Caccetta, P.A.; Zhou, Z.S.; McNeill, S.J.; Wu, X.; Mitchell, A.L. Joint Processing of Landsat and ALOS-PALSAR Data for Forest Mapping and Monitoring. *IEEE Trans. Geosci. Remote Sens.* **2011**, *50*, 55–67. [CrossRef]
4. Zhou, H.Z.; Qu, Z.L. The method to estimate timber volume with GIS in forest resouree inventory. *J. Northeast For. Univ.* **2000**, *28*, 50–53.
5. Zhang, K.; Hu, B. Individual Urban Tree Species Classification Using Very High Spatial Resolution Airborne Multi-Spectral Imagery Using Longitudinal Profiles. *Remote Sens.* **2012**, *4*, 1741–1757. [CrossRef]
6. Wang, L.; Fan, W.Y. Hyperspectral remote sensing data for identifying dominant forest tree species group. *J. Northeast For. Univ.* **2015**, *43*, 134–137.
7. Qian, H.S. Selection of the optimum temporal for crop estimation using remote sensing data: Main food crops in China. *Acta Ecol. Sin.* **1998**, *18*, 48–55.
8. Dahms, T.; Seissiger, S.; Borg, E.; Vajen, H.; Fichtelmann, B.; Conrad, C. Important Variables of a RapidEye Time Series for Modelling Biophysical Parameters of Winter Wheat. *Photogramm. Fernerkund. Geoinf.* **2016**, *5*, 285–299. [CrossRef]
9. Pan, Y.; Li, L.; Zhang, J.; Liang, S.; Zhu, X.; Sulla-Menashe, D. Winter wheat area estimation from MODIS-EVI time series data using the Crop Proportion Phenology Index. *Remote Sens. Environ.* **2012**, *119*, 232–242. [CrossRef]
10. Ou, W.; Su, W.; Xue, W.; Xia, X. Selection of optimum phase for yield estimation of three major crops based on HJ-1 satellite images. *Trans. CSAE* **2010**, *26*, 176–182.
11. Xu, G.C.; Pang, Y.; Li, Z.Y.; Zhao, K.R.; Liu, L.X. The changes of forest canopy spectral reflectance with seasons in Xiaoxing'anling. *Spectrosc. Spectr. Anal.* **2013**, *33*, 3303–3307.
12. Wang, W.J.; Zhang, X.; Zhao, Y.D.; Wang, S.D. Cotton extraction method of integrated multi-features basedon multi-temporal Landsat 8 images. *J. Remote Sens.* **2017**, *21*, 115–124.
13. Martin, M.E. Determining forest species composition using high spectral resolution remote sensing dates. *Remote Sens. Environ.* **1998**, *65*, 249–254. [CrossRef]
14. Tian, J.; Xing, Y.; Yao, S. Comparison of Landsat-TM Image Forest Type Classification Based on Cellular Automata and BP Neural Network Algorithm. *Sci. Silvae Sin.* **2017**, *53*, 26–34.
15. Zhang, J.; Zhang, X.; Tian, L.; Zhang, Q.F. The support vector machine method for RS images' classification in northwest arid area. *Sci. Surv. Mapp.* **2017**, *42*, 49–52. [CrossRef]

16. Li, D.R.; Wang, S.L.; Li, D.Y. *Spatial Data Mining Theory and Applications*, 2nd ed.; Science Press: Beijing, China, 2013.
17. Yue, J.; Wang, Z.X.; Feng, Z.F.; Li, Z.Y.; Wang, L.D. Studies on remote sensing recognition on fruit trees species based on spectrum and texture features in southern Xinjiang basin. *J. Xinjiang Agric. Univ.* **2015**, *38*, 326–333.
18. Zhang, Z.Y.; Liu, X.Y. Support vector machines for tree species identification using LiDAR-derived structure and intensity variables. *Geocarto Int.* **2013**, *28*, 364–378. [CrossRef]
19. Li, M.Y.; Xing, Y.Q.; Liu, M.S.; Wang, Z.; Yao, S.T.; Zeng, X.J.; Xie, J. Identification of forest type with Landsat-8 image based on SVM. *J. Cent. South Univ. For. Technol.* **2017**, *37*, 52–58.
20. Wang, L. *Satellite Remote Sensing Retrieval of Nitrogen and Phosphorous Nutritional Status in Apple Tree Leaves/Canopiesat Blossom Stage*; Shandong Agricultural University: Taian, China, 2012.
21. Yang, Y.L.; Cao, B.H.; Wu, D.; Zhang, D.P. The study of the main ornamental tree species resources of landscape forest on Mountan tai. *J. Inn. Mong. Agric. Univ. (Nat. Sci. Ed.)* **2007**, *28*, 19–24.
22. Liu, X.C.; Dai, Y.K.; Wang, X.Z. *Encyclopedia of Mount Tai*; Jinan, Shandong Friendship Publishing House: Jinan, China, 1995.
23. Institute of Geographical Research, Chinese Academy of Sciences. *Annual Report of Chinese Animal and Plant Phenological Observation (No. 9)*; Geological Publishing House: Beijing, China, 1989.
24. Cortes, C.; Vapnik, V. Support-vector networks. *Mach. Learn.* **1995**, *20*, 273–297. [CrossRef]
25. Wu, L.; Wen, Y. Weed/corn seedling recognition by support vector machine using texture features. *Afr. J. Agric. Res.* **2009**, *4*, 840–846.
26. Mathur, A.; Foody, G.M. Crop classification by support vector machine with intelligently selected training data for an operational application. *Int. J. Remote Sens.* **2008**, *29*, 2227–2240. [CrossRef]
27. Ahmed, F.; Bari, A.H.; Hossain, E.; Al-Mamun, H.A.; Kwan, P. Performance analysis of support vector machine and Bayesian classifier for crop and weed classification from digital images. *World Appl. Sci. J.* **2011**, *12*, 432–440.
28. Pulido, C.; Solaque, L.; Velasco, N. Weed recognition by SVM texture feature classification in outdoor vegetable crop images. *IngenIería InvestIgacIón* **2017**, *37*, 68–74. [CrossRef]
29. Ahmed, F.; Al-Mamun, H.A.; Bari, A.H.; Hossain, E.; Kwan, P. Classification of crops and weeds from digital images: A support vector machine approach. *Crop Prot.* **2012**, *40*, 98–104. [CrossRef]
30. Huang, H.; Liang, X.J.; Xiao, X.; Qiu, S.W.; Xiao, C.L.; Wang, Z. Model of groundwater quality assessment with support vector machine based on rough set. *China Environ. Sci.* **2016**, *36*, 619–625. [CrossRef]
31. Luo, J.C.; Zhou, C.H.; Leung, Y.; Ma, J.H. Support vector machine for spatial feature extraction and classification of remotely sensed imagery. *J. Remote Sens.* **2002**, *6*, 50–55.
32. Hogland, J.; Billor, N.; Anderson, N. Comparison of standard maximum likelihood classification and polytomous logistic regression used in remote sensing. *Eur. J. Remote Sens.* **2013**, *46*, 623–640. [CrossRef]
33. Meghanathan, N. Assortativity Analysis of Real-World Network Graphs based on Centrality Metrics. *Comput. Inf. Sci.* **2016**, *9*, 7. [CrossRef]
34. Evans, J.D. *Straightforward Statistics for the Behavioral Sciences*, 1st ed.; Brooks Cole Publishing Company: Salt Lake City, UT, USA, 1995.
35. Zhang, P.; Wang, H.; Wu, Q.; Yu, M.; Wu, T. Effect of wind on the relation of leaf N, P stoichiometry with leaf morphology in Quercus species. *Forests* **2018**, *9*, 110. [CrossRef]
36. Giovanetti, M.; Aronne, G. Honey bee handling behaviour on the papilionate flower of *Robinia pseudoacacia* L. *Arthropod-Plant Interact.* **2013**, *7*, 119–124. [CrossRef]